ChemPubSoc Europe

DOI: 10.1002/cctc.201600301

CHEMCATCHEM Communications

Inert Can Be Advantageous: Advisable Reconstruction and Application of Palladium Chloride for the Preferential Oxidation of the Hydrogen Impurity in Carbon Monoxide Streams

Luyang Qiao,[a] Qiaohong Li,[a] Zhangfeng Zhou,[a] Rui Si,[b] and Yuangen Yao*[a]

Preferential oxidation of the H_2 impurity in CO streams is crucial for the catalytic conversion of CO into ethylene glycol. It is uncertain as to whether H_2 can overthrow the dominance of CO and finally lead the reaction. Not only is this a typical research issue, but it is also extremely critical for practical applications. So far, no catalyst has shown selectivity higher than 50% owing to competitive adsorption of CO. In this work, we report a $PdCl_x$-based catalyst that can readily overcome the challenge mentioned above. Over this catalyst, the selectivity of H_2 oxidation is promoted by more than 40% relative to that over the conventional Pd/Al_2O_3 catalyst and reaches a value of 87%. The turnover frequency of undesired CO oxidation is inhibited by at least one order of magnitude. We found that the reconstructed palladium chloride was highly selective to this reaction by facile inhibition of the adsorption and oxidation of CO.

Through the coupling of CO to dimethyl oxalate and following selective hydrogenation,[1,2] the route for the catalytic conversion of CO into ethylene glycol has become a challenging and attractive subject of C_1 chemistry. As a raw material, CO is mainly derived from the reforming of abundant resources such as coal and shale gas. Nevertheless, desirable CO usually contains trace amounts of H_2 even after cryogenic separation, which is severely poisonous to the following process of CO coupling; thus, the amount of H_2 needs to be reduced to an acceptable level (below 100 ppm).[1b] To address this problem, the preferential oxidation (PrOx) of H_2 in a CO-rich stream was developed as the most promising approach among the chemical and physical methods. This technique is realized in the world's first plant of coal to ethylene glycol with a capacity of 200 000 tons (see Figure S1, Supporting Information).

H_2 oxidation is a common reaction that has been studied extensively as a model reaction and as an available method for H_2O_2 production.[3] Nevertheless, early studies on this reaction were generally performed under mild conditions, other than a competitive reactant-rich atmosphere, such as CO. As far as we know, research on the PrOx of H_2 in CO-rich streams is a largely unexplored area. The best catalyst ever manufactured for the PrOx of H_2 is Pd/Al_2O_3, which offers benchmarked performance and is highly active for H_2 conversion. Nevertheless, this catalyst is generally better able to oxidize CO than H_2 owing to the adsorption of CO on the metal surface, which significantly inhibits the adsorption and activation of H_2.[4,5] Depending on the feedback from a large-scale plant of coal to ethylene glycol, the selectivity for H_2 oxidation over the Pd/Al_2O_3 catalyst is generally lower than 50% despite the fact that the conversion of H_2 is high. Low selectivity inevitably induces the consumption of the CO feed and the accumulation of CO_2, both of which are not benign to subsequent dimethyl oxalate and ethylene glycol synthesis.

With the aim to elevate the selectivity, the rational design of novel catalysts based on fundamental understanding of this reaction is very critical. To drive the competitive reaction in a targeted direction, much effort has been dedicated to comprehending the effects of promoters by adjusting the structural or electronic texture of the catalyst.[6,7] However, another pathway to upgrade the selectivity by prohibiting the undesired side reaction has rarely been reported. Inhibitors can also be advantageous. Purposely exploiting a catalytically inert or even poisonous material towards one reaction can possibly proffer its counterpart certain enhanced effects. As a kind of well-known catalytic poison, chloride usually plays a negative role in the reaction of CO oxidation or PrOx.[8] Owing to the presence of chlorine, all the active sites on the catalyst will be occupied and the adsorption of the reactants will be blocked. This phenomenon provides us with some clues on how to promote the selectivity of H_2 oxidation by inhibiting the adsorption and oxidation of CO.

Herein, we first designed a $PdCl_x$-based catalyst that was verified to be highly selective towards the PrOx of H_2 in CO-rich streams. In contrast with the benchmark Pd/Al_2O_3 catalyst, CO oxidation was inhibited by at least one order of magnitude and the selectivity was promoted by more than 40% on the novel catalyst. It is proposed that the coordinatively unsaturat-

[a] Dr. L. Qiao, Dr. Q. Li, Dr. Z. Zhou, Prof. Y. Yao
Key Laboratory of Coal to Ethylene Glycol and Its Related Technology
State Key Laboratory of Structural Chemistry
Fujian Institute of Research on the Structure of Matter
Chinese Academy of Sciences
Yangqiao West Road 155
Fuzhou, Fujian 350002 (P.R. China)
E-mail: yyg@fjirsm.ac.cn

[b] Prof. R. Si
Shanghai Synchrotron Radiation Facility
Shanghai Institute of Applied Physics
Chinese Academy of Sciences
Shanghai 201204 (P.R. China)

Supporting Information for this article can be found under: http://dx.doi.org/10.1002/cctc.201600301.

ed (CU) configuration of $PdCl_x$ is responsible for this breakthrough. By intentionally reconstructing the texture of palladium chloride, the best balance of activity and selectivity was achieved. The catalyst (denoted as CU-$PdCl_x/Al_2O_3$) was prepared by incipient wetness impregnation. For comparison, the $PdCl_2/Al_2O_3$ and Pd/Al_2O_3 catalyst were also prepared. The Pd loadings of all the discussed catalysts were measured by inductively coupled plasma optical emission spectrometry (ICP-OES) and were found to be between 0.9 and 1.1 wt%, which correspond well to theoretical values. The BET surface areas of all the discussed catalysts were slightly lower than that of the bare Al_2O_3 support (310 $m^2 g^{-1}$) owing to pore blocking by impregnation (see Table S1).

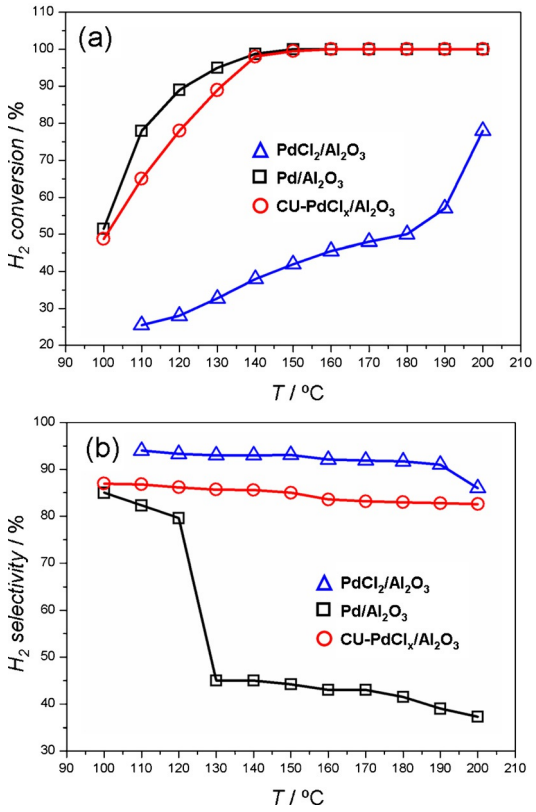

Figure 1. a) Conversion of H_2 and b) selectivity for H_2 oxidation as a function of reaction temperature over the CU-$PdCl_x/Al_2O_3$, Pd-Al_2O_3, and $PdCl_2/Al_2O_3$ catalysts.

The properties of the catalysts were evaluated under simulated industrial conditions (2 vol% H_2, 4 vol% O_2, and 94 vol% CO).[9] As the most efficient catalyst ever manufactured for the PrOx of H_2, Pd/Al_2O_3 was initially tested to benchmark the activity and selectivity of the system. Figure 1a illustrates the profiles of the H_2 conversions as a function of reaction temperature. The conversion of H_2 approximated to 50% at 100 °C and reached 100% at 150 °C over Pd/Al_2O_3. With a similar tendency, the H_2 conversion over CU-$PdCl_x/Al_2O_3$ reached 99.5% at 150 °C, and the complete oxidation of H_2 was realized at 155 °C. However, the activity of $PdCl_2/Al_2O_3$ was much lower than that of CU-$PdCl_x/Al_2O_3$. The conversion of H_2 was negligible at 100 °C and decreased to 50% at 180 °C. This can probably be attributed to the relative intact structure of $PdCl_2$, and therefore, the adsorption of the reactants is significantly hindered.

The selectivities are compared in Figure 1b. For Pd/Al_2O_3, the selectivity approached a maximum at 100 °C, and then abruptly decreased to 44.2% upon increasing the temperature to 150 °C. At this temperature, complete conversion of H_2 was achieved at the expense of the selectivity, which suggested that CO oxidation began to predominate the system. In contrast, the selectivity of CU-$PdCl_x/Al_2O_3$ initially attained 87% at 100 °C, and this level was steadily maintained over the entire temperature region with a slight decrease of only 5%. This result is significantly better than that on Pd/Al_2O_3 and indicates that the oxidation of CO is probably inhibited efficiently on CU-$PdCl_x/Al_2O_3$. In addition, the selectivity of $PdCl_2/Al_2O_3$ was the highest, but this is meaningless owing to its low activity for the desired reaction.

To further demonstrate the extraordinarily high selectivity of H_2 oxidation over CU-$PdCl_x/Al_2O_3$, the catalytic behavior of the catalysts were examined from the viewpoint of kinetics. The turnover frequency (TOF) values of the catalysts for all the reactions were measured under different conditions (conversions below 20%) and are shown in Table 1. For H_2 oxidation in a CO-rich stream, the TOF for H_2 conversion over CU-$PdCl_x/Al_2O_3$ was 4.8×10^{-2} s^{-1} at 90 °C, which approximates to that over Pd/Al_2O_3; this indicates that both catalysts are able to oxi-

Table 1. Turnover frequencies and apparent activation energies over the CU-$PdCl_x/Al_2O_3$ and Pd/Al_2O_3 catalysts for the PrOx of H_2 in a CO-rich stream and CO oxidation in the presence of H_2 at different temperatures.

Sample	H_2 oxidation in CO-rich stream			CO oxidation in the presence of H_2		
	T [°C]	TOF $\times10^{-2}$ [s^{-1}][a]	E_a [kJ mol^{-1}]	T [°C]	TOF $\times10^{-2}$ [s^{-1}][a]	E_a [kJ mol^{-1}]
CU-$PdCl_x/Al_2O_3$	60	1.8	29.9	110	0.6	38.6
	70	2.8		130	1.1	
	80	3.7		150	2.1	
	90	4.8		170	3.2	
Pd/Al_2O_3	60	2.4	24.9	110	18.6	3.8
	70	3.2		130	19.8	
	80	4.1		150	20.9	
	90	5.0		170	21.9	

[a] The dispersion of Pd was measured by CO chemisorption by using a Micromeritics ASAP 2020 M+C by assuming CO/Pd = 1:1.

dize H_2. For CO oxidation in the presence of H_2, the TOF for CO conversion was only 0.6×10^{-2} s^{-1} at 110 °C. Relative to that on Pd/Al_2O_3, the TOF on CU-$PdCl_x/Al_2O_3$ is almost 30-fold lower under the same conditions. This inhibition indicates that it is difficult to oxidize CO over CU-$PdCl_x/Al_2O_3$. On the basis of the Arrhenius plots (Figure S5), we calculated the apparent activation energies (E_a) of the CU-$PdCl_x/Al_2O_3$ and Pd/Al_2O_3 catalysts. The E_a value of 38.6 kJ mol^{-1} over CU-$PdCl_x/Al_2O_3$ is one order of magnitude higher than that of 3.8 kJ mol^{-1} over Pd/Al_2O_3 for CO oxidation. The high activation barrier of CU-$PdCl_x/Al_2O_3$ correlates well with its efficient inhibition of CO oxidation and outstanding selectivity towards H_2 oxidation.

Previous studies illustrated that the presence of CO usually has a negative effect on reactions in which H_2 is involved.[10,11] To investigate the influence of a high concentration of CO on the PrOx of H_2, we tested the adsorption behavior of the catalysts by static chemisorption. In the individual tests, Table S2 shows that the adsorption of both H_2 and CO on Pd/Al_2O_3 is more facile than on CU-$PdCl_x/Al_2O_3$. Relative to the amount of CO adsorbed without competition of H_2, the amount of CO adsorbed slightly decreased on both CU-$PdCl_x/Al_2O_3$ (from 24.5 to 18.8 μmol g^{-1}) and Pd/Al_2O_3 (from 43 to 34.6 μmol g^{-1}) after H_2 preadsorption. With a reverse order of CO/H_2 adsorption, however, the behavior of these two catalysts was very different. After CO preadsorption, a significant decrease (from 24.6 to 5.9 μmol g^{-1}) in the amount of H_2 adsorbed was observed on Pd/Al_2O_3. This indicates that a strong interaction between CO and the Pd sites is established on Pd/Al_2O_3, and then the adsorption of H_2 is blocked. On the contrary, only a small decrease (from 14.3 to13 μmol g^{-1}) in the amount of H_2 adsorbed was found on CU-$PdCl_x/Al_2O_3$. The coordination of Cl around the Pd sites should be responsible for this result, as this tends to deplete backdonation from the d bands of Pd to the antibonding $2\pi^*$ orbitals of CO.[12] Thus, the interaction between CO and Pd is weakened. Such fragile adsorption of CO on the catalyst makes CO labile and commutable by H_2. Finally, the adsorption gap between CO and H_2 can be minimized over CU-$PdCl_x/Al_2O_3$ by deliberately restricting access to CO, and then the opportunity for H_2 is maximized.

Both the electronic properties and the short-range local structures of the discussed catalysts were determined from the extended X-ray absorption fine structure (EXAFS) spectra and X-ray absorption near-edge structure (XANES) spectra of the Pd K-edge. As shown in Figure 2a, the XANES curve of $PdCl_2/Al_2O_3$ fits well with the standard $PdCl_2$ sample, but a slight deviation is found in CU-$PdCl_x/Al_2O_3$, which suggests that the local electron density of Pd increases as the coordination of electron-withdrawing Cl becomes unsaturated. This verifies that the intrinsic structure of $PdCl_x$ is not intact. In contrast, the curve of Pd/Al_2O_3 shows two metallic peaks at energies of approximately 24367 and 24391 eV. These features are identical to those of a standard Pd foil sample.

The curves of the Fourier-transformed k^2-weighted Pd K-edge EXAFS are shown in Figure 2b. The Pd–Cl coordination number (CN) of CU-$PdCl_x/Al_2O_3$ (3.3 ± 0.4) is markedly lower than that of the standard $PdCl_2$ sample and that of $PdCl_2/Al_2O_3$ (5.3 ± 0.9), and the Pd–Cl distance (R) of $PdCl_x$ is smaller, which

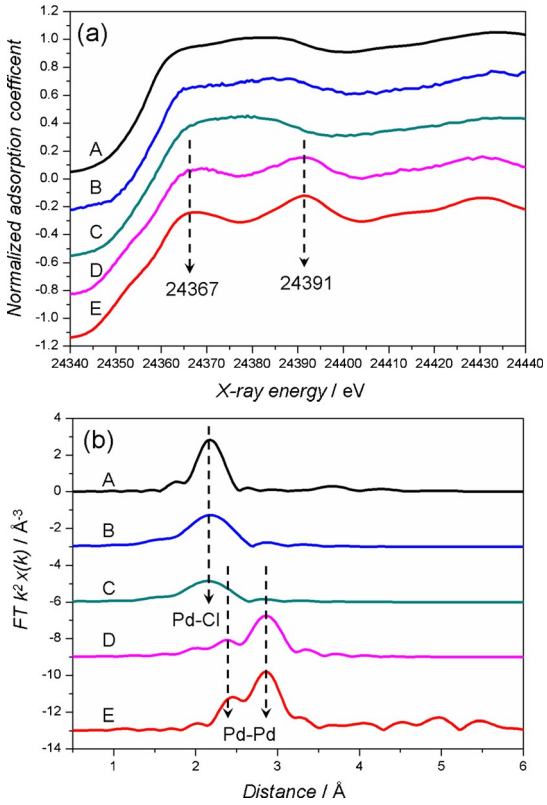

Figure 2. a) XANES spectra and b) k^2-weighted Fourier transform Pd K-edge EXAFS spectra of the standard $PdCl_2$ power (A), $PdCl_2/Al_2O_3$ (B), CU-$PdCl_x/Al_2O_3$ (C), Pd/Al_2O_3 (D), and standard Pd foil (E).

suggests that the Pd–Cl bond increases in length as the amount of excess Cl decreases and the configuration of $PdCl_x$ becomes coordinatively unsaturated. Besides that, no Pd–Pd bond can be detected in CU-$PdCl_x/Al_2O_3$, and consequently, no metallic Pd particles are formed.

Notably, the E_a values acquired from the Arrhenius plots are apparent in that the diffusional effect was not eliminated; therefore, an intrinsic investigation about the behavior of the catalysts is essential. DFT calculations were performed to explore the inhibitory mechanisms of CO oxidation over the $PdCl_x$ structure. The chosen Pd (111) surface of Pd/Al_2O_3 and the defective $PdCl_x$ (140) surface of CU-$PdCl_x/Al_2O_3$ were identified through characterization by high-resolution transmission electron microscopy, X-ray absorption fine structure, and X-ray photoelectron spectroscopy (see Section S6 in the Supporting Information). The comparable energetic landscapes of all the pathways for CO oxidation on the surfaces are depicted in Schemes S2 and S3. We propose two mechanisms for CO oxidation depending on whether H_2 is involved or not.

On Pd (111), pathway I is illustrated by a redox mechanism in which H_2 is only a spectator.[13] As shown in Figure 3, adsorbed CO* is directly attacked by O_2 to yield a carbonate intermediate (CO_3*) with a barrier of 1.66 eV via transition state 1 (TS1), and it then decomposes to CO_2 and O* via TS2. CO_2 is readily desorbed from the Pd surface and O* approaches another adsorbed CO* species to produce another molecule of CO_2 via TS3. Differing in the adsorption modes, other similar

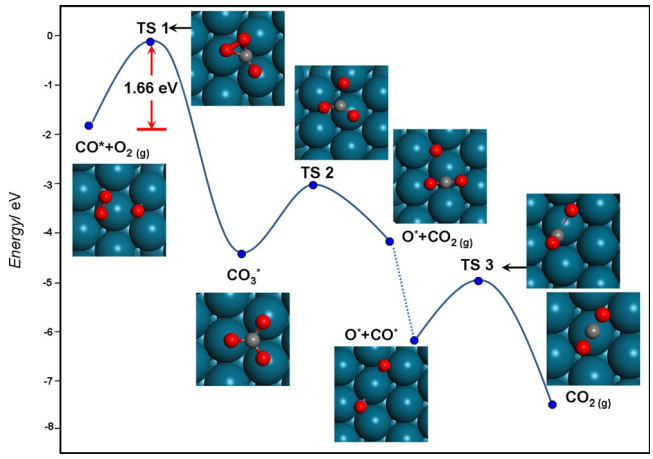

Figure 3. Pathway I for CO oxidation on the Pd (111) surface with TS1–TS3.

pathways were also investigated (see Section S5.2). Although the barriers for these other pathways are slightly lower than that for pathway I, the odds that they will occur are low, because their initial states are contradicted by the real circumstances of our system. With the involvement of H_2, an associate mechanism is proposed in pathway II. As shown in Figure 4,

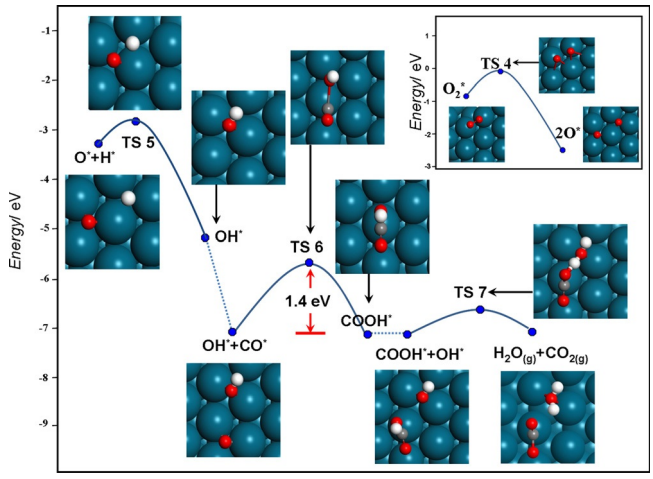

Figure 4. Pathway II for CO oxidation on the Pd (111) surface with TS4–TS7.

adsorbed O_2* initially dissociates into two O* (TS4), own of which abstracts H* to form hydroxy groups (OH*) on the Pd (111) surface via TS5. Then, one OH* associates with CO* to yield a carboxylate intermediate (OCOH*) via TS6 by overcoming a barrier of 1.4 eV. Finally, this OCOH* species transfers a hydrogen atom to another neighboring OH* spontaneously to yield CO_2 and H_2O via TS7, in which a long OCOHOH* intermediate geometry is formed, as previously speculated by Ojifinni et al.[14] The lower barrier of pathway II indicates that CO oxidation is probably enhanced by participation of H_2. This effect is assisted by the initial formation of OH*, which is supported by studies on hydroxy-enhanced CO oxidation and the water–gas shift reaction.[15,16]

On $PdCl_x$ (140), on the basis of our calculations all the proposed pathways need to overcome a higher energy barrier. As shown in Figure 5, preferred pathway II for CO oxidation was comparatively investigated on this surface. Initially, two dissociated H* grasp gaseous O_2 to form a HOOH* species (other

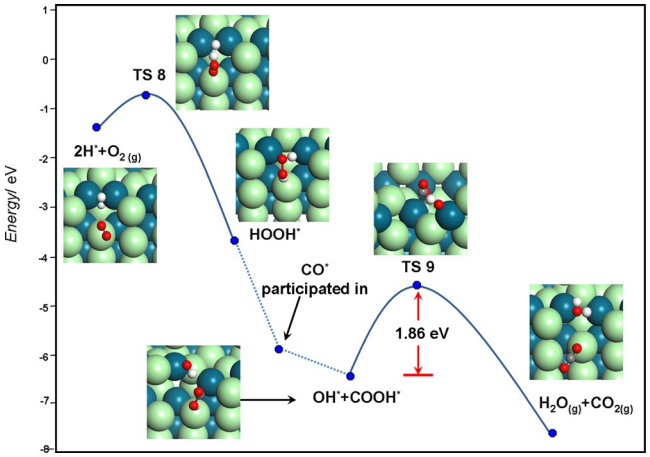

Figure 5. Pathway II for CO oxidation on the $PdCl_x$ (140) surface with TS8 and TS9.

than OH*) on the defective sites (V_{Cl}) via TS8 owing to the lack of exposed Pd. Then, adsorbed CO* readily substitutes a hydroxy group in HOOH* to yield a OCOH* intermediate. If this replaced OH* intends to associate with OCOH* again to abstract a hydrogen atom, a higher barrier of 1.86 eV must be surmounted via TS9. Besides that, the barrier of pathway I, which abides by a redox mechanism, also increases from 1.66 to 2.71 eV on the $PdCl_x$ (140) surface. This indicates that the oxidation of CO is undoubtedly inhibited on the $PdCl_x$ (140) surface, regardless of whether H_2 is involved or not.

We then performed in situ diffuse reflectance infrared Fourier transform spectroscopy (DRIFTS) experiments to further verify the inhibitory mechanisms proposed by DFT calculations. The spectra of CO oxidation in the presence of H_2 were recorded in the range of 40 to 200 °C over the discussed catalysts. For clarity, only the region of 3000 to 1150 cm^{-1} is extracted for detailed illustration. As shown in Figure S6, injecting the reactants into the cell initially yielded CO bands of the gaseous type ($\tilde{\nu}$ = 2173 and 2120 cm^{-1}), linear type ($\tilde{\nu}$ = 2090 cm^{-1}), and bridged type ($\tilde{\nu}$ = 1968 cm^{-1}) at 40 °C.[17] Furthermore, bands at $\tilde{\nu}$ = 1435 and 1230 cm^{-1} were also observed, and they were generally attributed to the O–C–O stretching vibration of the CO_3* species.[18] With an increase in the temperature, a series of new bands ($\tilde{\nu}$ = 1596, 1396, 1374 cm^{-1}) corresponding to the O–C–O stretching vibration of the OCOH* species[19] emerged and became clearer above 130 °C. Simultaneously, the intensities of the bands associated with the CO_3* species gradually decreased as the new bands emerged. This suggested that the associate mechanism began to dominate the reaction. Coupled with maximization of the OCOH* species, the bands for CO_2 ($\tilde{\nu}$ = 2362 and 2342 cm^{-1})[15a] abruptly increased in intensity and remained almost steady in the range of 130 to

200 °C. The dramatic increase in the intensity of the CO_2 bands indicates that the oxidation of CO is enhanced by the participation of H_2 through pathway II.

For CU-$PdCl_x/Al_2O_3$, the spectra depicted in Figure 6 exhibit certain differences upon comparison to the spectra of Pd/Al_2O_3. The bands of the OCOH* or CO_3* intermediate are not observed over the entire range of temperatures, which indicates that all the pathways for CO oxidation abiding by an associate or redox mechanism do not occur. Furthermore, the intensity of the CO_2 signal is approximately only 1/20 of that on Pd/Al_2O_3. This wide margin unequivocally demonstrates that CO oxidation is inhibited by at least one order of magnitude on CU-$PdCl_x/Al_2O_3$, which correlates well with our DFT calculations.

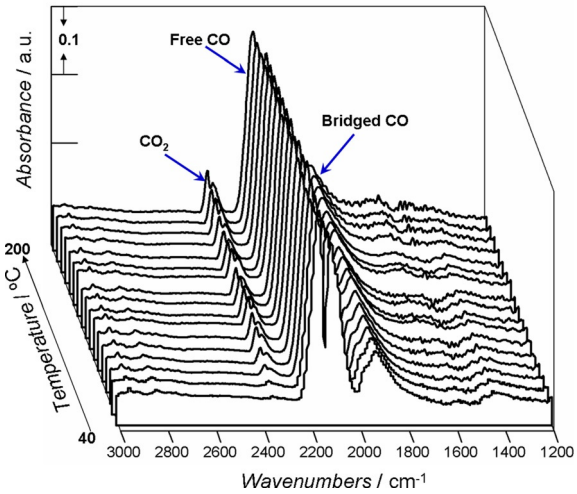

Figure 6. In situ DRIFTS spectra for CO oxidation in the presence of H_2 over the CU-$PdCl_x/Al_2O_3$ catalyst.

In conclusion, we developed a highly efficient CU-$PdCl_x/Al_2O_3$ catalyst for the abatement of the H_2 impurity in CO streams. Relative to that on the conventional Pd/Al_2O_3 catalyst, the selectivity for H_2 oxidation on CU-$PdCl_x/Al_2O_3$ is significantly higher and is increased by more than 40%, and furthermore, the conversion of H_2 is ensured. Hence, the best balance of activity and selectivity could be acquired over this catalyst. We demonstrated that the superior performance of this catalyst could be attributed to the dual inhibitory effects of $PdCl_x$ for CO adsorption and oxidation. By exploring the mechanism of this structure-guided behavior, we found that the energy barrier for all favored pathways for CO oxidation were difficult to overcome on the $PdCl_x$ (1 4 0) surface. We believe that insight into the unconventional utilization of catalytically inert palladium chloride to promote this reaction will give researchers some clues for the rational design of catalysts and will allow us to reconsider that an inert, even poisonous, material for one reaction may play an inverse role for its counterpart.

Experimental Section

All catalysts were prepared by incipient wetness impregnation. Typically, commercial γ-Al_2O_3 (2 g) was impregnated into an aqueous solution of $PdCl_2$ (10 mL, Aldrich, 99.9%) at an appropriate concentration at 25 °C for 6 h. The pH value of the solution was controlled at pH ≈ 2 by adding hydrochloric acid. After impregnation, the sample was dried at 100 °C under vacuum for 12 h and was then treated in a microwave reactor for 10 min. The patterned $PdCl_2/Al_2O_3$ catalyst was thus obtained. We treated this catalyst (1 g) with 0.5 vol% aqueous vapor and 10 vol% H_2 balanced with Ar under 150 °C for 30 min. The resulting catalyst was denoted CU-$PdCl_x/Al_2O_3$. With the same procedures, the patterned Pd/Al_2O_3 catalyst was also synthesized by replacing $PdCl_2$ with $Pd(NO_3)_2$ (Aldrich, 99.9%), and the sample was reduced further under 200 °C with 10 vol% H_2/Ar mixture. Details of the catalytic measurements, characterization data, and DFT calculations are given in the Supporting Information.

Acknowledgements

The authors are thankful for financial support from the 973 Program of China (2011CBA00505), the Strategic Priority Research Program of the Chinese Academy of Sciences (XDA07070200 and XDA09030102), and the National Key Technology R&D Program (2012BAE06B08). The work was also supported by the BL14W1 beam line of the Shanghai Synchrotron Radiation Facility.

Keywords: C1 building blocks · hydrogen · oxidation · palladium · selectivity

[1] a) Q. Li, Z. Zhou, R. Chen, B. Sun, L. Qiao, Y. Yao, K. Wu, *Phys. Chem. Chem. Phys.* **2015**, *17*, 9126 – 9134; b) S. Peng, Z. Xu, Q. Chen, Y. Chen, J. Sun, Z. Wang, M. Wang, G. Guo, *Chem. Commun.* **2013**, *49*, 5718 – 5720.

[2] a) Z. He, H. Lin, P. He, Y. Yuan, *J. Catal.* **2011**, *277*, 54 – 63; b) Y. Huang, H. Ariga, X. Zheng, X. Duan, S. Takakusagi, K. Asakura, Y. Yuan, *J. Catal.* **2013**, *307*, 74 – 83.

[3] a) L. Ouyang, P. Tian, G. Da, X. Xu, C. Ao, T. Chen, R. Si, J. Xu, Y. Han, *J. Catal.* **2015**, *321*, 70 – 80; b) T. R. Reina, C. Megias-Sayago, A. P. Florez, S. Ivanova, M. A. Centeno, J. A. Odriozola, *J. Catal.* **2015**, *326*, 161 – 171.

[4] a) T. Schalow, B. Brandt, D. E. Starr, M. Laurin, S. K. Shaikhutdinov, S. Schauermann, J. Libuda, H. J. Freund, *Angew. Chem. Int. Ed.* **2006**, *45*, 3693 – 3697; *Angew. Chem.* **2006**, *118*, 3775 – 3780; b) H. J. Freund, G. Meijer, M. Scheffler, R. Schlogl, M. Wolf, *Angew. Chem. Int. Ed.* **2011**, *50*, 10064 – 10094; *Angew. Chem.* **2011**, *123*, 10242 – 10275.

[5] a) H. Conrad, G. Ertl, E. E. Latta, *J. Catal.* **1974**, *35*, 363 – 368; b) R. J. Behm, V. Penka, M. G. Cattania, K. Christmann, G. Ertl, *J. Chem. Phys.* **1983**, *78*, 7486 – 7490; c) G. A. Kok, A. Noordemeer, B. E. Nieuwenhuys, *Surf. Sci.* **1983**, *135*, 65 – 80.

[6] a) P. Sonström, D. Arndt, X. Wang, V. Zielasek, M. Baumer, *Angew. Chem. Int. Ed.* **2011**, *50*, 3888 – 3891; *Angew. Chem.* **2011**, *123*, 3974 – 3978; b) S. Colussi, A. Gayen, M. F. Camellone, M. Boaro, J. Llorca, S. Fabris, A. Trovarelli, *Angew. Chem. Int. Ed.* **2009**, *48*, 8481 – 8484; *Angew. Chem.* **2009**, *121*, 8633 – 8636.

[7] a) C. Zhang, F. Liu, Y. Zhai, H. Ariga, N. Yi, Y. Liu, K. Asakura, M. Flytzani-Stephanopoulos, H. He, *Angew. Chem. Int. Ed.* **2012**, *51*, 9628 – 9632; *Angew. Chem.* **2012**, *124*, 9766 – 9770; b) N. Ji, T. Zhang, M. Zheng, A. Wang, H. Wang, X. Wang, J. Chen, *Angew. Chem. Int. Ed.* **2008**, *47*, 8510 – 8513; *Angew. Chem.* **2008**, *120*, 8638 – 8641.

[8] a) H. S. Oh, J. H. Yang, C. K. Costello, Y. Wang, S. R. Bare, H. H. Kung, M. C. Kung, *J. Catal.* **2002**, *210*, 375 – 386; b) A. Wootsch, C. Descorme, D. Duprez, *J. Catal.* **2004**, *225*, 259 – 266.

[9] a) Y. Yao, China Patent., ZL201110181697.3, **2011**; b) Y. Yao, China Patent., ZL201110182739.5, **2011**.

[10] a) M. Morkel, G. Rupprechter, H. J. Freund, *J. Chem. Phys.* **2003**, *119*, 10853 – 10866; b) J. M. White, S. Akther, *CRC Crit. Rev. Solid State Mater. Sci.* **1988**, *14*, 131.
[11] a) M. Eriksson, L. C. Ekedahl, *Surf. Sci.* **1998**, *412*, 430 – 440; b) C. Nyberg, L. Westerlund, *Surf. Sci.* **1991**, *256*, 9 – 18.
[12] G. Blyholder, *J. Phys. Chem.* **1964**, *68*, 2772.
[13] a) T. Bunluesin, R. J. Gorte, G. W. Graham, *Appl. Catal. B* **1998**, *15*, 107 – 114; b) G. Chinchen, M. Spencer, *J. Catal.* **1988**, *112*, 325 – 327.
[14] R. A. Ojifinni, N. S. Froemming, J. Gong, M. Pan, T. S. Kim, J. M. White, G. Henkelman, C. B. Mullins, *J. Am. Chem. Soc.* **2008**, *130*, 6801 – 6812.
[15] a) J. Lin, B. Qiao, L. Li, H. Guan, C. Ruan, A. Wang, W. Zhang, X. Wang, T. Zhang, *J. Catal.* **2014**, *319*, 142 – 149; b) J. Lin, B. Qiao, J. Liu, Y. Huang, A. Wang, L. Li, W. Zhang, L. Allard, X. Wang, T. Zhang, *Angew. Chem. Int. Ed.* **2012**, *51*, 2920 – 2924; *Angew. Chem.* **2012**, *124*, 2974 – 2978.
[16] a) M. Yang, J. L. Liu, S. Lee, B. Zugic, J. Huang, L. F. Allard, M. Flytzani-Stephanopoulos, *J. Am. Chem. Soc.* **2015**, *137*, 3470 – 3473; b) G. G. Olympiou, C. M. Kalamaras, C. D. Zeinalipour-Yazdi, A. M. Efstathiou, *Catal. Today* **2007**, *127*, 304 – 318.
[17] K. I. Choi, M. A. Vannice, *J. Catal.* **1991**, *127*, 465 – 488.
[18] a) X. Liu, W. Ruettinger, X. Xu, R. Farrauto, *Appl. Catal. B* **2005**, *56*, 69 – 75; b) K. G. Azzam, I. V. Babich, K. Seshan, L. Lefferts, *J. Catal.* **2007**, *251*, 153 – 162.
[19] a) C. M. Kalamaras, S. Americanou, A. M. Efstathiou, *J. Catal.* **2011**, *279*, 287 – 300; b) G. Jacobs, B. H. Davis, *Appl. Catal. A* **2007**, *333*, 192 – 20.

Received: March 15, 2016
Published online on May 23, 2016